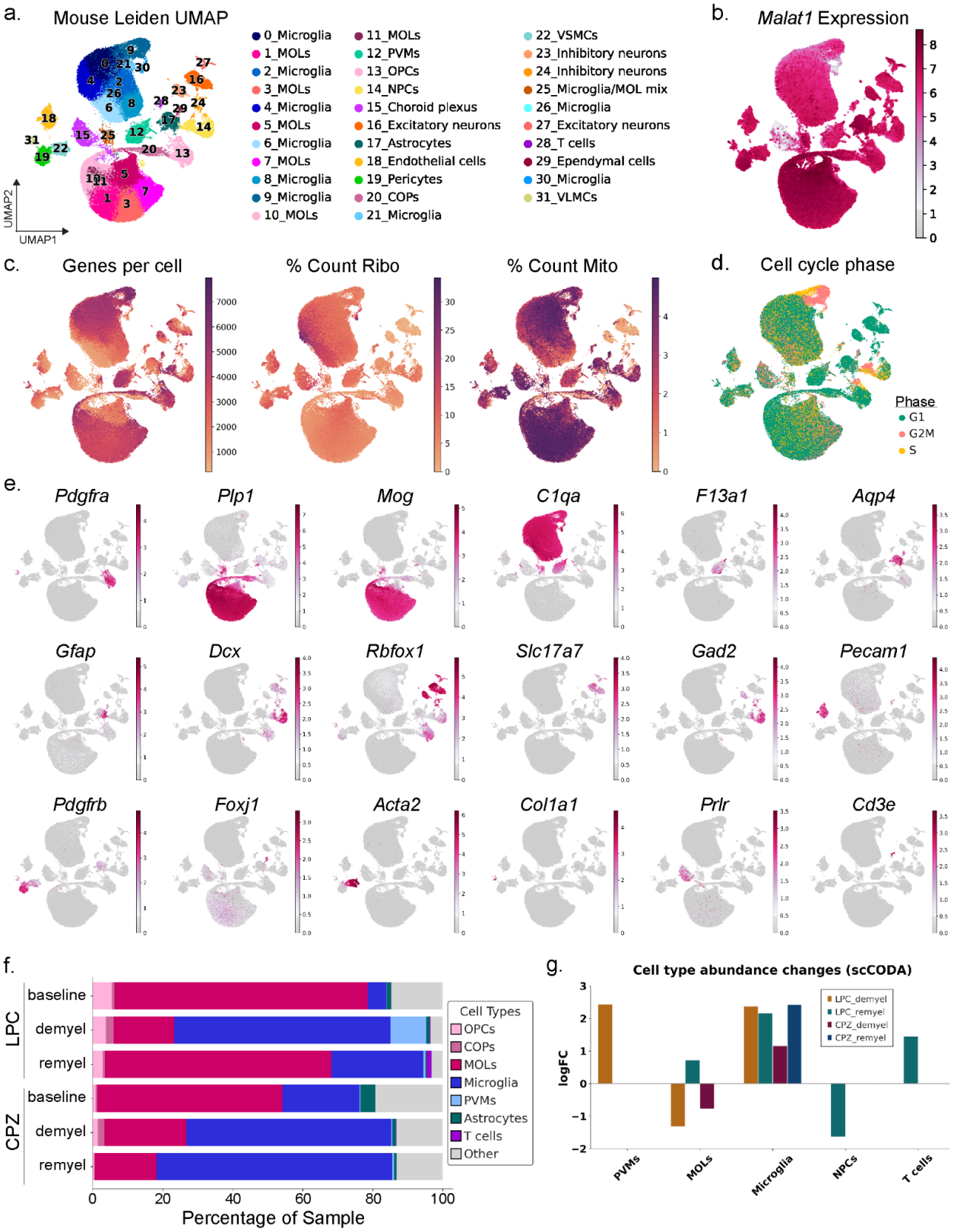
a.
Mouse Leiden UMAP
0_Microglia
1_MOLs
2_Microglia
3_MOLs
4_Microglia
5_MOLs
6_Microglia
7_MOLs
8_Microglia
9_Microglia
10_MOLs
11_MOLs
12_PVMs
13_OPCs
14_NPCs
15_Choroid plexus
16_Excitatory neurons
17_Astrocytes
18_Endothelial cells
19_Pericytes
20_COPs
21_Microglia
22_VSMCs
23_Inhibitory neurons
24_Inhibitory neurons
25_Microglia/MOL mix
26_Microglia
27_Excitatory neurons
28_T cells
29_Ependymal cells
30_Microglia
31_VLMCs
UMAP2
UMAP1
b.
Malat1 Expression
c.
Genes per cell
% Count Ribo
% Count Mito
d.
Cell cycle phase
Phase
G1
G2M
S
e.
Pdgfra
Plp1
Mog
C1qa
F13a1
Aqp4
Gfap
Dcx
Rbfox1
Slc17a7
Gad2
Pecam1
Pdgfrb
Foxj1
Acta2
Col1a1
Prlr
Cd3e
f.
LPC
CPZ
baseline
demyel
remyel
Cell Types
OPCs
COPs
MOLs
Microglia
PVMs
Astrocytes
T cells
Other
Percentage of Sample
g.
Cell type abundance changes (scCODA)
logFC
LPC_demyel
LPC_remyel
CPZ_demyel
CPZ_remyel
PVMs
MOLs
Microglia
NPCs
T cells

Supplementary Figure 1: Quality control of mouse data.

a. UMAP of the fully integrated mouse dataset, with cell types labeled based on Leiden clustering.
b. UMAP showing *Malat1* expression, where low expression serves as a proxy for low-quality cells.
c. UMAPs displaying key quality control metrics, including genes per cell, % ribosomal counts (% Count Ribo), and % mitochondrial counts (% Count Mito).
d. Cell-cycle phase analysis plotted on the integrated UMAP. Three actively dividing cell populations are identified, corresponding to OPCs, microglia, and NPCs.
e. UMAPs showing the expression of the indicated marker genes, corresponding to the dot plot in Figure 1c.
f. Stacked bar chart showing the distribution of annotated cell types across each timepoint. Corresponding metadata is available in Supplemental Data 1.
g. Bar chart depicting the significant cell compositional changes calculated by scCODA. Calculations were made per condition and compared to the respective baseline. Pericytes were used as the reference cell type.

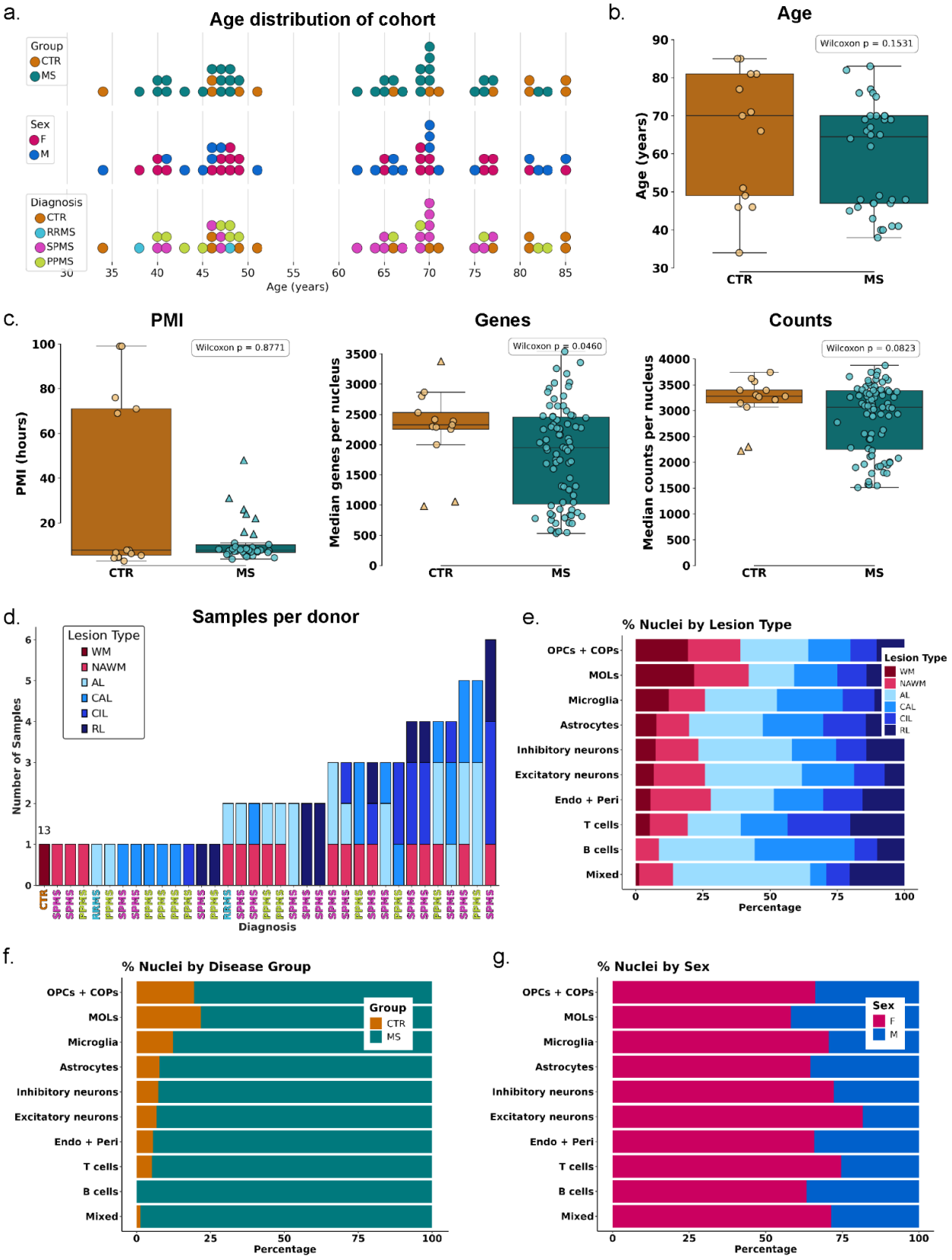
a.
Age distribution of cohort
Group
CTR
MS
Sex
F
M
Diagnosis
CTR
RRMS
SPMS
PPMS
Age (years)
b.
Age
Wilcoxon p = 0.1531
Age (years)
CTR
MS
c.
PMI
Wilcoxon p = 0.8771
PMI (hours)
Genes
Wilcoxon p = 0.0460
Median genes per nucleus
Counts
Wilcoxon p = 0.0823
Median counts per nucleus
d.
Samples per donor
Lesion Type
WM
NAWM
AL
CAL
CIL
RL
Number of Samples
Diagnosis
e.
% Nuclei by Lesion Type
OPCs + COPs
MOLs
Microglia
Astrocytes
Inhibitory neurons
Excitatory neurons
Endo + Peri
T cells
B cells
Mixed
Percentage
f.
% Nuclei by Disease Group
Group
CTR
MS
g.
% Nuclei by Sex
Sex
F
M

Supplementary Figure 2: Statistical comparison and quality control of human metadata.

a. Age distribution of patient cohort, colored by group (control (CTR) and MS patients (top), sex (female (F), male (M), middle) and diagnosis (relapse-remitting MS (RRMS), secondary progressive MS (SPMS) and primary progressive MS (PPMS), bottom).
b. Box plot showing the age distribution of CTR and MS patient donors. As the data was not normally distributed (confirmed using the Shapiro-Wilk test), a Mann-Whitney U test was used to compare the groups and indicated no significant difference. The boxes represent the interquartile range (IQR), with the center line showing the median. Whiskers extend to the most extreme data points within 1.5 × IQR from the lower (Q1) and upper (Q3) quartiles. All individual donor ages are shown as points.
c. Box plot (as in b), showing the postmortem interval (PMI), median number of genes per nucleus, and median counts per nucleus across donor samples in CTR and MS groups. Outliers, identified using the IQR method, are shown as triangles. As the data were not normally distributed, a Mann-Whitney U test was used. A statistically significant difference was observed between groups for PMI and genes per nucleus.
d. Stacked bar chart showing the number of unique samples per donor. Each bar represents one patient and is colored by lesion type, except for the 13 controls (Ctr) represented by 1 bar. The x-axis shows the patient diagnoses (SP: secondary progressive, PP: primary progressive, RR: relapse remitting). For MS patients, thirteen individuals contributed one sample and 21 individuals contributed more than one sample.
e. Stacked bar chart showing the percentage contribution to the respective cell type cluster color by lesion type.
f. Stacked bar chart showing the percentage contribution to the respective cell type cluster colored by group.
g. Stacked bar chart showing the percentage contribution to the respective cell type cluster colored by sex.

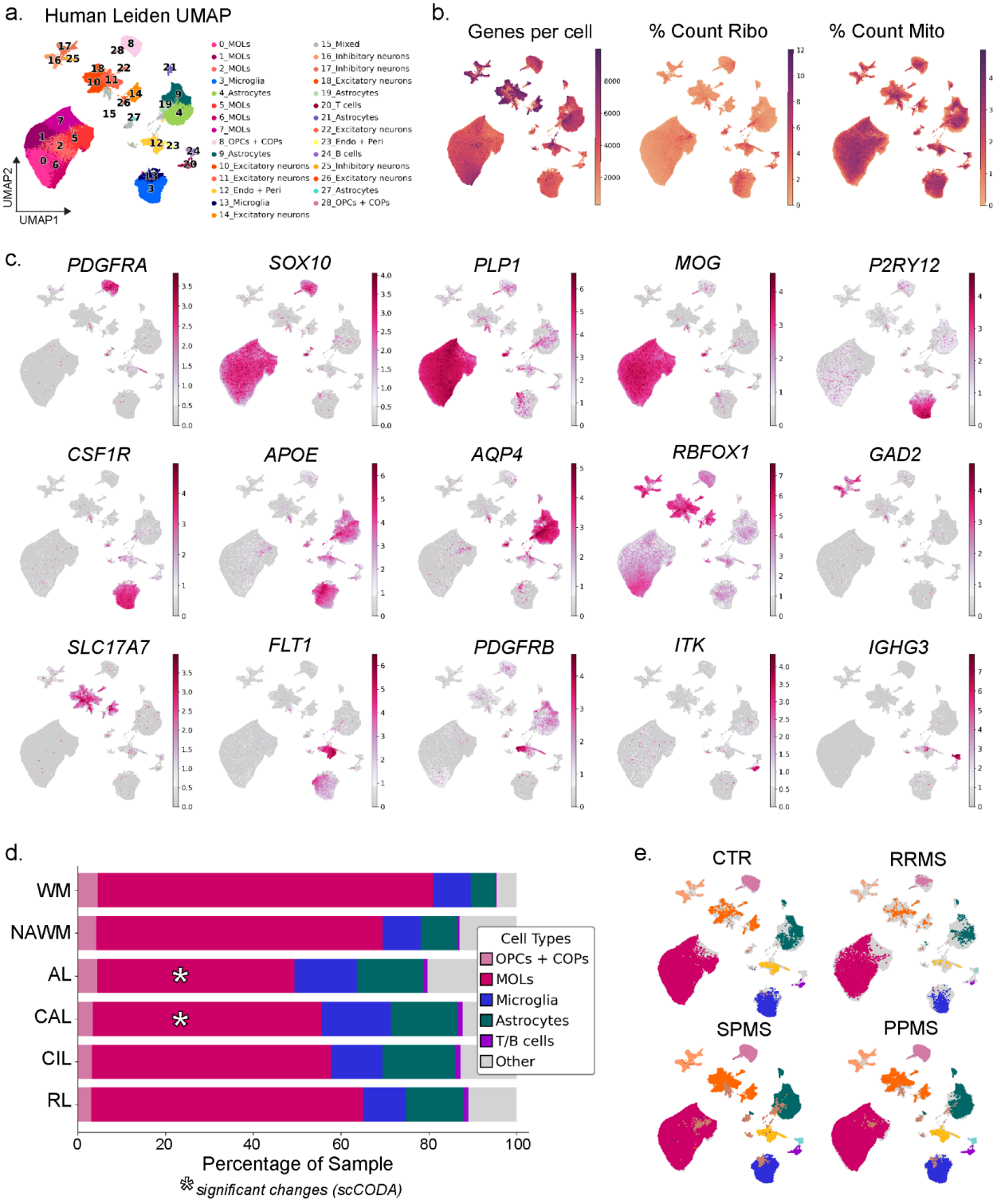
a.
Human Leiden UMAP
UMAP2
UMAP1
0_MOLs
1_MOLs
2_MOLs
3_Microglia
4_Astrocytes
5_MOLs
6_MOLs
7_MOLs
8_OPCs + COPs
9_Astrocytes
10_Excitatory neurons
11_Excitatory neurons
12_Endo + Peri
13_Microglia
14_Excitatory neurons
15_Mixed
16_Inhibitory neurons
17_Inhibitory neurons
18_Excitatory neurons
19_Astrocytes
20_T cells
21_Astrocytes
22_Excitatory neurons
23_Endo + Peri
24_B cells
25_Inhibitory neurons
26_Excitatory neurons
27_Astrocytes
28_OPCs + COPs
b.
Genes per cell
% Count Ribo
% Count Mito
c.
PDGFRA
SOX10
PLP1
MOG
P2RY12
CSF1R
APOE
AQP4
RBFOX1
GAD2
SLC17A7
FLT1
PDGFRB
ITK
IGHG3
d.
WM
NAWM
AL
CAL
CIL
RL
Cell Types
OPCs + COPs
MOLs
Microglia
Astrocytes
T/B cells
Other
Percentage of Sample
significant changes (scCODA)
e.
CTR
RRMS
SPMS
PPMS

Supplementary Figure 3: Quality control of integration from human samples.

a. UMAP of the integrated dataset, with cell types labeled based on Leiden clustering.
b. UMAPs displaying key quality control metrics, including genes per nucleus, % ribosomal counts (% Count Ribo), and % mitochondrial counts (% Count Mito).
c. UMAPs showing expression of the indicated marker genes, corresponding to the dot plot in Figure 1g.
d. Stacked bar chart showing the proportion of glial cell types per lesion type. (Other = neurons, Endo + Peri, and mixed cell types). Asterisks denote significant compositional changes calculated using scCODA by comparing each lesion type to WM and using the cluster “Endo + Peri” as the reference cell type.
e. UMAPs separated by disease status (Ctr: control, RRMS: relapse remitting MS, SPMS: secondary progressive MS, PPMS: primary progressive MS).

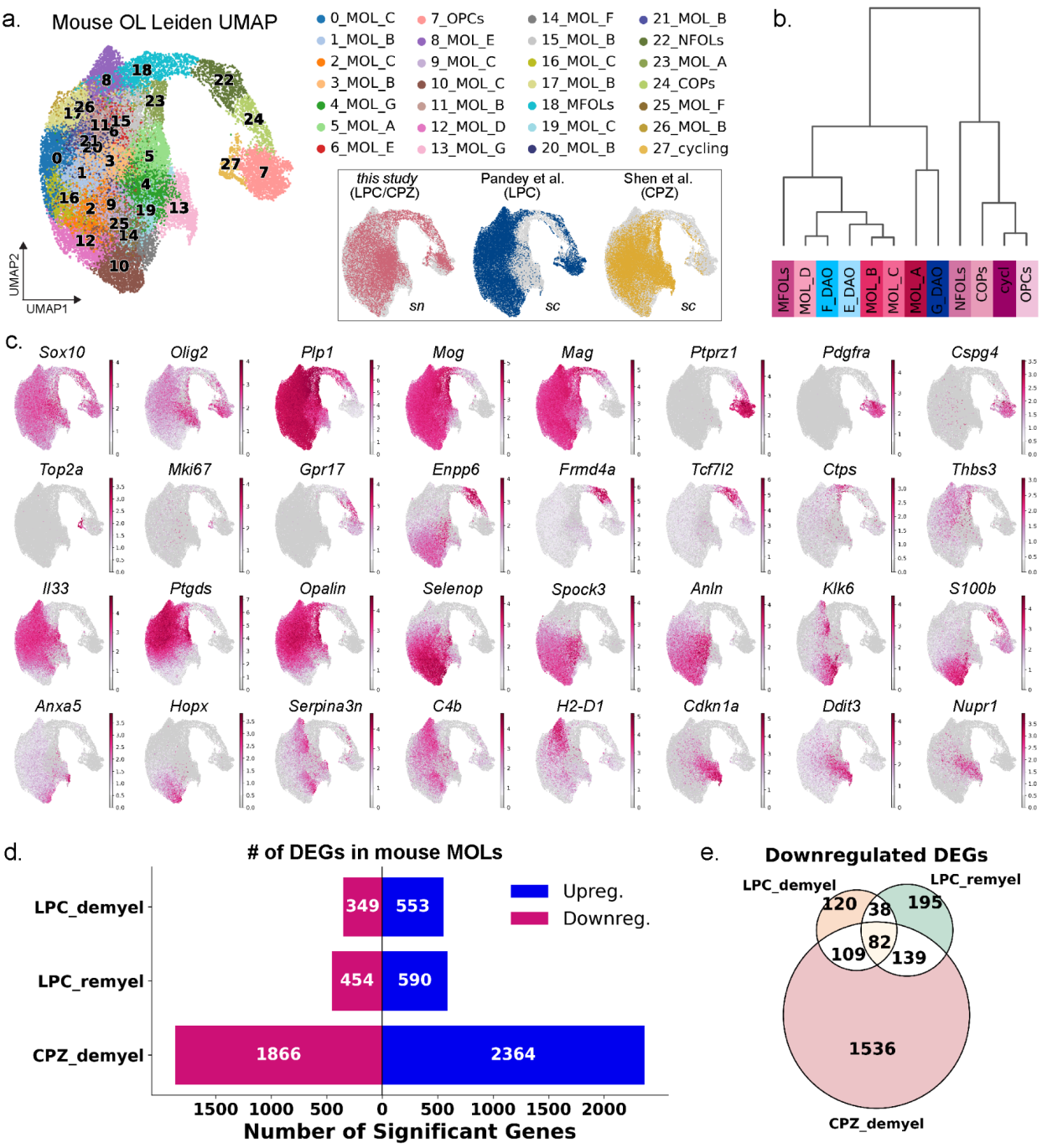
a.
Mouse OL Leiden UMAP
UMAP2
UMAP1
0_MOL_C
1_MOL_B
2_MOL_C
3_MOL_B
4_MOL_G
5_MOL_A
6_MOL_E
7_OPCs
8_MOL_E
9_MOL_C
10_MOL_C
11_MOL_B
12_MOL_D
13_MOL_G
14_MOL_F
15_MOL_B
16_MOL_C
17_MOL_B
18_MFOLs
19_MOL_C
20_MOL_B
21_MOL_B
22_NFOLs
23_MOL_A
24_COPs
25_MOL_F
26_MOL_B
27_cycling
this study (LPC/CPZ)
Pandey et al. (LPC)
Shen et al. (CPZ)
sn
sc
sc
b.
MFOLs
MOL_D
F_DAO
E_DAO
MOL_B
MOL_C
MOL_A
G_DAO
NFOLs
COPs
cycl
OPCs
c.
Sox10
Olig2
Plp1
Mog
Mag
Ptprz1
Pdgfra
Cspg4
Top2a
Mki67
Gpr17
Enpp6
Frmd4a
Tcf7l2
Ctps
Thbs3
Il33
Ptgds
Opalin
Selenop
Spock3
Anln
Klk6
S100b
Anxa5
Hopx
Serpina3n
C4b
H2-D1
Cdkn1a
Ddit3
Nupr1
d.
# of DEGs in mouse MOLs
LPC_demyel
LPC_remyel
CPZ_demyel
349
553
454
590
1866
2364
Upreg.
Downreg.
1500 1000 500 0 500 1000 1500 2000
Number of Significant Genes
e.
Downregulated DEGs
LPC_demyel
LPC_remyel
CPZ_demyel
120
38
195
109
82
139
1536

Supplementary Figure 4: Mouse oligodendrocyte lineage clustering, marker expression, and differential expression analysis.

a. UMAP of the OL subset, with cell types labeled based on Leiden clustering. Inset UMAPs show samples separated and colored by dataset origin, labeled by demyelination paradigm and sequencing type.
b. Dendrogram showing the hierarchical clustering of the cell types, colored as in the UMAP in Figure 2a.
c. UMAPs showing expression of the indicated marker genes, corresponding to the dot plot in Figure 2b.
d. Stacked bar chart showing the upregulated (blue) and downregulated (magenta) differentially expressed genes (DEGs) in the indicated cell type and timepoint.
e. Venn diagram illustrating the unique and overlapping significantly downregulated genes (fold change ≤ –1.5, *padj* < 0.05) calculated from the pseudobulk of all MOLs in LPC or CPZ at demyelination, and LPC at remyelination.

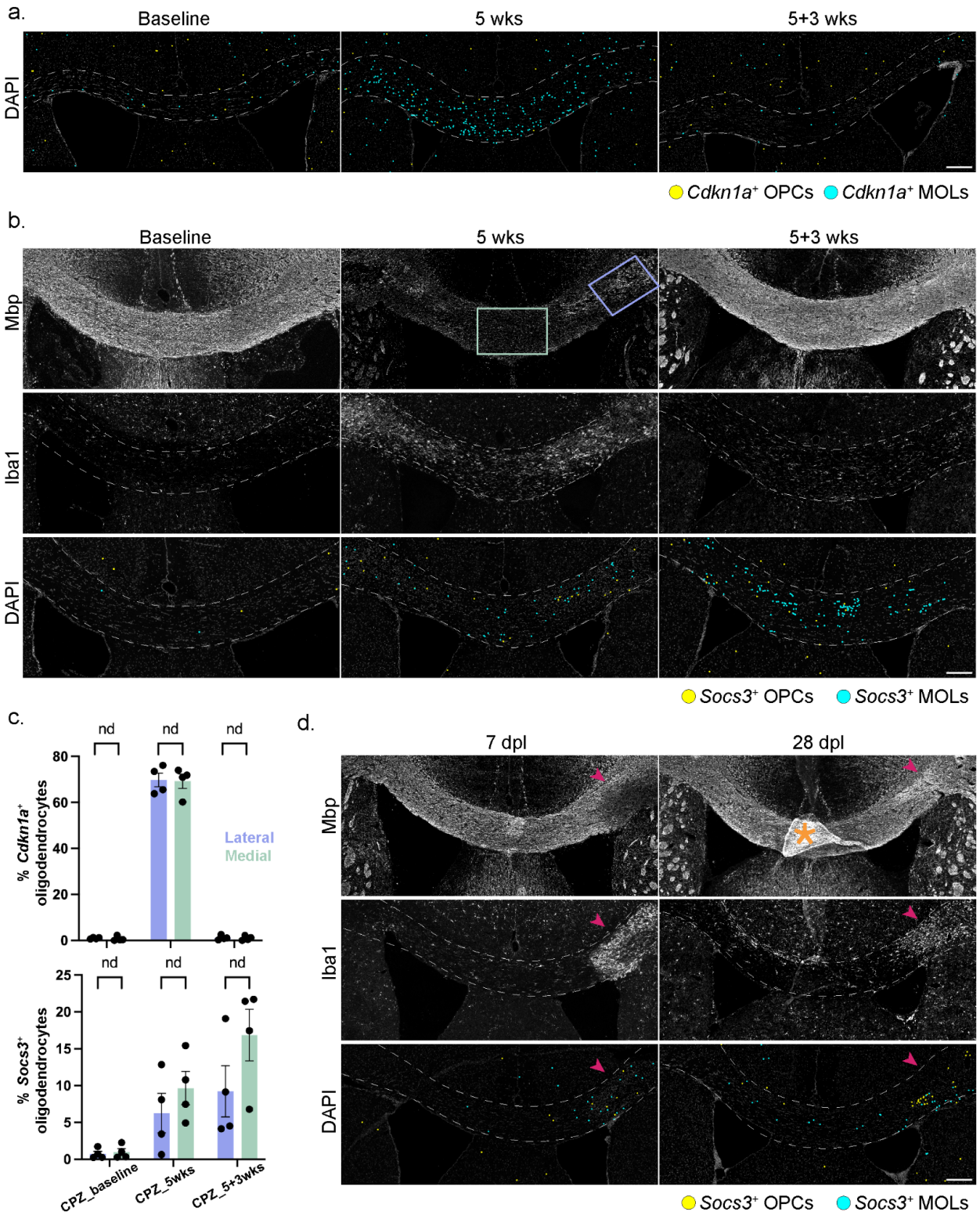
a.
Baseline
5 wks
5+3 wks
DAPI
Cdkn1a+ OPCs
Cdkn1a+ MOLs
b.
Baseline
5 wks
5+3 wks
Mbp
Iba1
DAPI
Socs3+ OPCs
Socs3+ MOLs
c.
nd
% Cdkn1a+ oligodendrocytes
Lateral
Medial
% Socs3+ oligodendrocytes
CPZ_baseline
CPZ_5wks
CPZ_5+3wks
d.
7 dpl
28 dpl
Mbp
Iba1
DAPI
Socs3+ OPCs
Socs3+ MOLs

Supplementary Figure 5: Spatial distribution of LPC and CPZ DAO phenotypes.

a. Representative tiled 40× RNAscope/IHC images of coronal mouse brain sections following CPZ administration at the indicated timepoints. Nuclei are labeled with DAPI (white) and colored dots indicate *Cdkn1a*$^{+}$ OPCs (yellow) and *Cdkn1a*$^{+}$ MOLs (cyan). Dashed white lines outline the corpus callosum. (Scale bar=200 μm).
b. Representative tiled 40× IHC images across serial sections of the indicated CPZ timepoints showing Mbp (top), Iba1 (middle), and RNAscope/IHC detection of *Socs3*$^{+}$ OPCs (yellow) and *Socs3*$^{+}$ MOLs (cyan) shown against DAPI-labeled nuclei (white, bottom). Cell identities are defined as in (a). Dashed lines outline the corpus callosum. Purple and green boxes denote lateral and medial regions, respectively, used for spatial quantification of DAOs. (Scale bar=200 μm).
c. Quantification of the spatial distribution (lateral vs. medial corpus callosum) of *Cdkn1a*$^{+}$ (top) and *Socs3*$^{+}$ (bottom) MOLs in baseline and CPZ-induced demyelination and remyelination. Bars show group means, dots show individual animals, and error bars represent the standard error of the mean (SEM). No significant differences were detected across regions at any timepoint (unpaired Welch's t-test and FDR of 1%).
d. Representative tiled 40× IHC images, shown as in (b), across serial sections from LPC-injected mice. Magenta arrowheads indicate the LPC injection site; saline was injected on the contralateral side. The orange asterisk marks a tissue fold (non-biological artifact of the tissue processing). (Scale bar=200 μm).

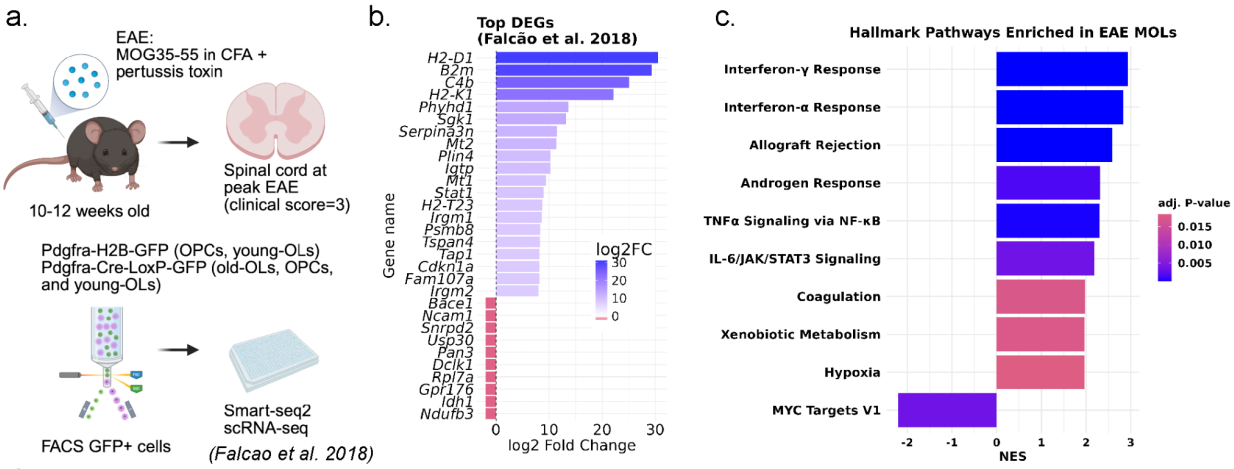
a.
EAE:
MOG35-55 in CFA +
pertussis toxin
10-12 weeks old
Spinal cord at
peak EAE
(clinical score=3)
Pdgfra-H2B-GFP (OPCs, young-OLs)
Pdgfra-Cre-LoxP-GFP (old-OLs, OPCs,
and young-OLs)
FACS GFP+ cells
Smart-seq2
scRNA-seq
(Falcao et al. 2018)
b.
Top DEGs
(Falcão et al. 2018)
H2-D1
B2m
C4b
H2-K1
Phyhd1
Sgk1
Serpina3n
Mt2
Plin4
Iqtp
Mt1
Stat1
H2-T23
Irgm1
Psmb8
Tspan4
Tap1
Cdkn1a
Fam107a
Irgm2
Bace1
Ncam1
Snrpd2
Usp30
Pan3
Dclk1
Rpl7a
Gpr176
Idh1
Ndufb3
Gene name
log2FC
30
20
10
0
0
10
20
30
log2 Fold Change
c.
Hallmark Pathways Enriched in EAE MOLs
Interferon-γ Response
Interferon-α Response
Allograft Rejection
Androgen Response
TNFα Signaling via NF-κB
IL-6/JAK/STAT3 Signaling
Coagulation
Xenobiotic Metabolism
Hypoxia
MYC Targets V1
adj. P-value
0.015
0.010
0.005
-2
-1
0
1
2
3
NES

d.

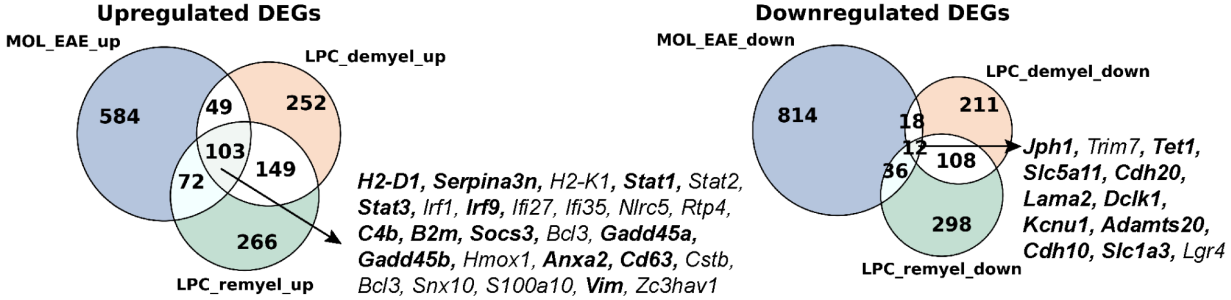
Upregulated DEGs
MOL_EAE_up
LPC_demyel_up
LPC_remyel_up
584
49
252
103
149
72
266
H2-D1, Serpina3n, H2-K1, Stat1, Stat2,
Stat3, Irf1, Irf9, Ifi27, Ifi35, Nlrc5, Rtp4,
C4b, B2m, Socs3, Bcl3, Gadd45a,
Gadd45b, Hmox1, Anxa2, Cd63, Cstb,
Bcl3, Snx10, S100a10, Vim, Zc3hav1
Downregulated DEGs
MOL_EAE_down
LPC_demyel_down
LPC_remyel_down
814
18
211
12
108
36
298
Jph1, Trim7, Tet1,
Slc5a11, Cdh20,
Lama2, Dclk1,
Kcnu1, Adamts20,
Cdh10, Slc1a3, Lgr4

e.

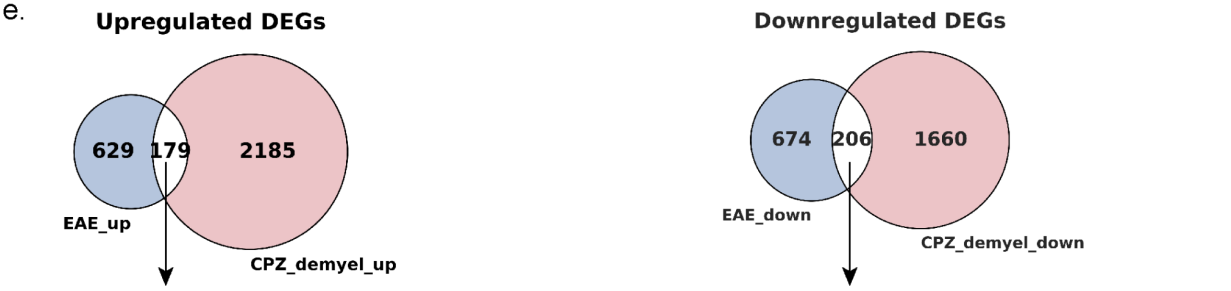
Upregulated DEGs
629
179
2185
EAE_up
CPZ_demyel_up
H2-D1, B2m, Serpina3n, Tap2, Stat1, Stat3, Irf3, Irf9,
Parp3, C4b, Ddx24, Ddx52, Psmd13, Psmd2, Gadd45a,
Gadd45b, Socs3, Cebpd, Cdkn1a, Cd63, Rhoj, Rasip1,
Rgs20, Anxa2, Vim, Parp12
Downregulated DEGs
674
206
1660
EAE_down
CPZ_demyel_down
Dnmt3a, Hdac11, Tet1, S100b, Il18, Gprc5b,
Abhd12, Slc1a3, Ncam1, Dclk1, Gpr155, Usp30
Gpr176, Fsd1l, Ncoa3, Tspan15, Pan3, Stard5

Supplementary Figure 6: Comparison of LPC and CPZ gene expression changes with a mouse EAE model.

a. Schematic of the EAE dataset used for comparison. EAE was induced in transgenic adult mice that label OPCs and OLs with GFP. At the peak of the disease, mice were sacrificed and spinal cord OPCs and OLs were FACS sorted. Single-cell RNA-seq data was collected using a plate-based protocol called Smart-seq2. Created in Biorender. Aboelnour, E. (2026) https://BioRender.com/p6zimjt.
b. Bar chart of the top upregulated and downregulated genes from the EAE dataset. The provided supplementary table of DEGs from the original manuscript, calculated using MAST, includes only significant DEGs with a logFC of at least 1.5-fold.
c. Bar chart showing the enrichment of Hallmark pathways in the EAE dataset. Ranking score was set to the logFC, as this is the only available data for the DEG list provided from the original manuscript. Color indicates the *padj*-value and bar length is the normalized enrichment score (NES).
d. Overlap of upregulated (left) and downregulated (right) genes between EAE and LPC oligodendrocytes. A subset of genes is listed from the intersection of all 3 datasets. Bolded genes are shared between LPC, CPZ and EAE.
e. Overlap of upregulated (left) and downregulated (right) genes between EAE and CPZ oligodendrocytes. A subset of genes is listed from the intersection of all 3 datasets. Bolded genes are shared between LPC, CPZ and EAE.

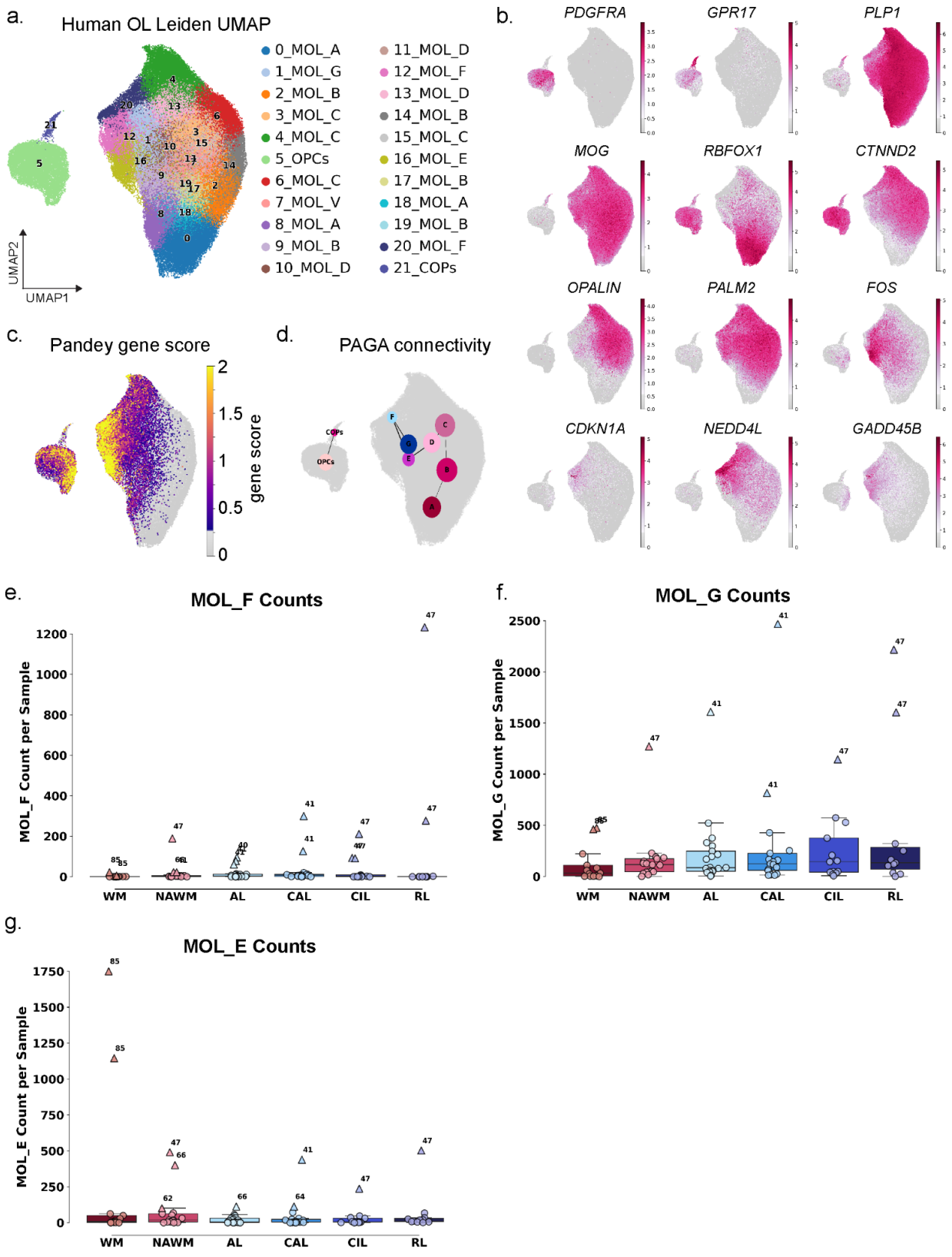
a.
Human OL Leiden UMAP
0_MOL_A
1_MOL_G
2_MOL_B
3_MOL_C
4_MOL_C
5_OPCs
6_MOL_C
7_MOL_V
8_MOL_A
9_MOL_B
10_MOL_D
11_MOL_D
12_MOL_F
13_MOL_D
14_MOL_B
15_MOL_C
16_MOL_E
17_MOL_B
18_MOL_A
19_MOL_B
20_MOL_F
21_COPs
UMAP2
UMAP1
b.
PDGFRA
GPR17
PLP1
MOG
RBFOX1
CTNND2
OPALIN
PALM2
FOS
CDKN1A
NEDD4L
GADD45B
c.
Pandey gene score
gene score
d.
PAGA connectivity
COPs
OPCs
e.
MOL_F Counts
MOL_F Count per Sample
f.
MOL_G Counts
MOL_G Count per Sample
g.
MOL_E Counts
MOL_E Count per Sample
WM
NAWM
AL
CAL
CIL
RL

Supplementary Figure 7: Human oligodendrocyte lineage clustering, marker expression and QC.

a. UMAP of the human oligodendrocyte lineage, with cell types labeled based on Leiden clustering.
b. UMAPs showing expression of the indicated marker genes, corresponding to the dot plot in Figure 4b.
c. Gene scores calculated using the expression of DAO genes identified by Pandey et al. in mouse models that are conserved in MS patient samples (genes listed in Methods).
d. UMAP showing PAGA connectivity with edge weights above 0.25 between the annotated cell types as shown in Figure 4a.
e. Box plots of MOL_F cell type count across lesion types, with each dot representing a single sample. Triangles indicate samples identified as statistical outliers based on interquartile range (IQR), defined as samples exceeding 1.5× IQR above the third quartile. Outliers are annotated with the age at death of the donor in years.
f. Box plots of MOL_G cell type count across lesion types, presented as in (e).
g. Box plots of MOL_E cell type count across lesion types, presented as in (e).

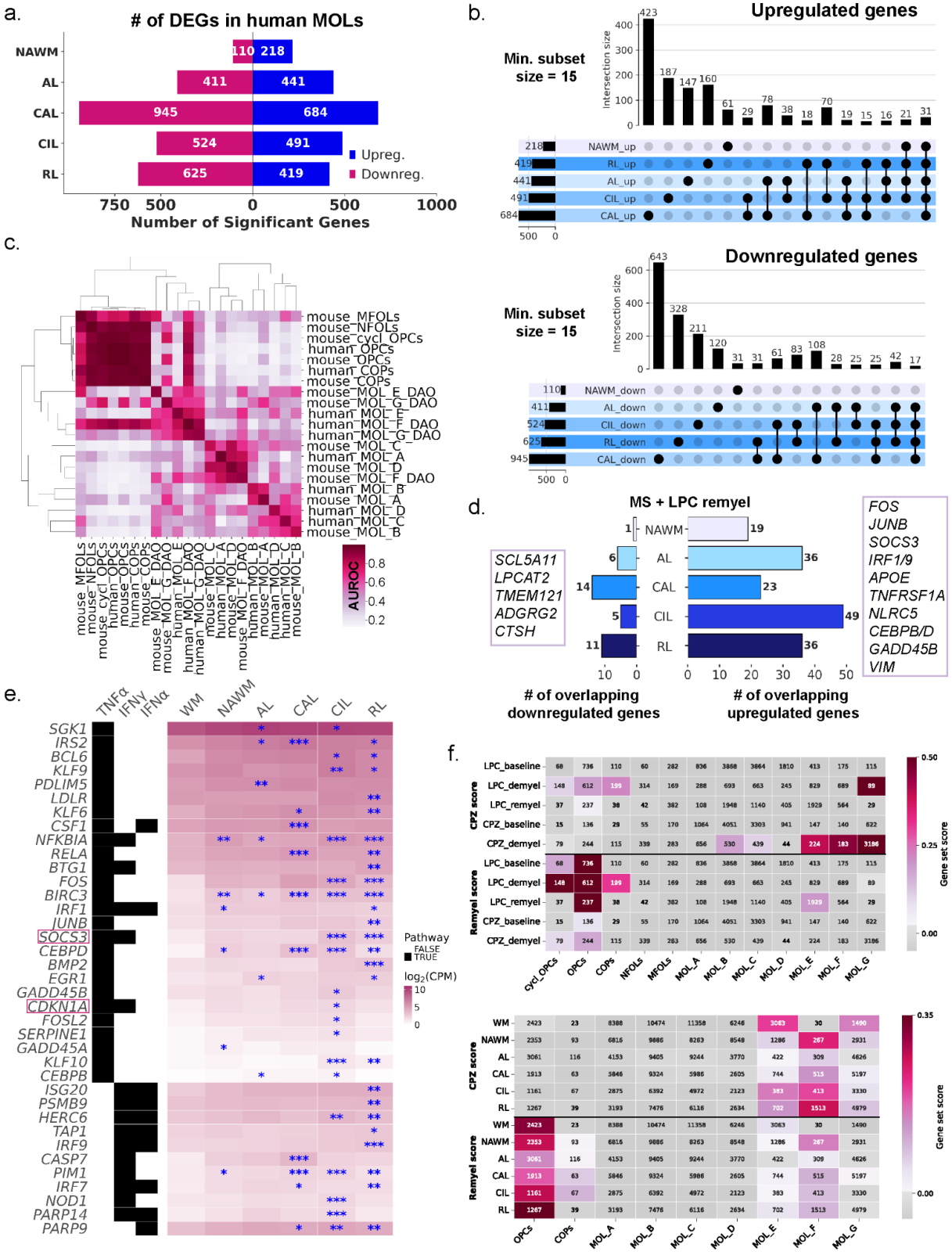
a.
# of DEGs in human MOLs
NAWM
AL
CAL
CIL
RL
110
218
411
441
945
684
524
491
625
419
Upreg.
Downreg.
750 500 0 500 1000
Number of Significant Genes
b.
Upregulated genes
Min. subset size = 15
Intersection size
423
187
147
160
61
29
78
38
18
70
19
15
16
21
31
NAWM_up
RL_up
AL_up
CIL_up
CAL_up
218
419
441
491
684
500 0
Downregulated genes
Min. subset size = 15
643
328
211
120
31
31
61
83
108
28
25
25
42
17
NAWM_down
AL_down
CIL_down
RL_down
CAL_down
110
411
524
625
945
500 0
c.
mouse_MFOLs
mouse_NFOLs
mouse_cycl_OPCs
human_OPCs
mouse_OPCs
human_COPs
mouse_COPs
mouse_MOL_E_DAO
mouse_MOL_G_DAO
human_MOL_E
human_MOL_F_DAO
human_MOL_G_DAO
mouse_MOL_C
human_MOL_A
mouse_MOL_D
mouse_MOL_F_DAO
human_MOL_B
mouse_MOL_A
human_MOL_D
human_MOL_C
mouse_MOL_B
AUROC
0.8
0.6
0.4
0.2
d.
MS + LPC remyel
SCL5A11
LPCAT2
TMEM121
ADGRG2
CTSH
NAWM
AL
CAL
CIL
RL
1
6
14
5
11
19
36
23
49
36
10 0
0 10 20 30 40 50
# of overlapping downregulated genes
# of overlapping upregulated genes
FOS
JUNB
SOCS3
IRF1/9
APOE
TNFRSF1A
NLRC5
CEBPB/D
GADD45B
VIM
e.
TNFα
IFNγ
IFNα
WM
NAWM
AL
CAL
CIL
RL
SGK1
IRS2
BCL6
KLF9
PDLIM5
LDLR
KLF6
CSF1
NFKBIA
RELA
BTG1
FOS
BIRC3
IRF1
JUNB
SOCS3
CEBPD
BMP2
EGR1
GADD45B
CDKN1A
FOSL2
SERPINE1
GADD45A
KLF10
CEBPB
ISG20
PSMB9
HERC6
TAP1
IRF9
CASP7
PIM1
IRF7
NOD1
PARP14
PARP9
Pathway
FALSE
TRUE
log2(CPM)
10
5
0
f.
CPZ score
Remyel score
LPC_baseline
LPC_demyel
LPC_remyel
CPZ_baseline
CPZ_demyel
cycl_OPCs
OPCs
COPs
NFOLs
MFOLs
MOL_A
MOL_B
MOL_C
MOL_D
MOL_E
MOL_F
MOL_G
Gene set score
0.50
0.25
0.00
WM
NAWM
AL
CAL
CIL
RL
0.35
0.00

Supplementary Figure 8: Human oligodendrocyte DEG analysis and comparison with mouse models.

a. Stacked bar chart showing the total number of upregulated (blue) and downregulated (magenta) DEGs across all MOLs per lesion type.
b. UpSet plots showing the unique (single points) and overlapping (connected points) DEGs in MOLs across lesion conditions that are upregulated (fold change ≥ 1.5, padj < 0.05, top) and downregulated (fold change ≤ –1.5, padj < 0.05, bottom). Overlap size was filtered to include only points with 15 or more shared genes.
c. Heatmap of AUROC scores between mouse and human OL lineage cells calculated using MetaNeighbor analysis. Dendrograms were generated by hierarchical clustering of Euclidean distances using average linkage.
d. Bar chart showing the overlap of upregulated and downregulated DEGs shared between MOLs in the mouse LPC remyelination timepoint and the MS lesions. Some genes that are shared between LPC remyelination MOLs and at least one MS lesion type are shown beside the down and upregulated bars.
e. Heatmap showing expression of genes in the indicated pathways across lesion conditions. Heatmaps are colored by the average $\log_2$-transformed CPM expression values. Gene–pathway associations were assigned to pathways using the Hallmark sets and are shown in the left annotation panel, where black tiles indicate pathway membership. Genes are hierarchically ordered first by pathway inclusion and then by average expression across all conditions. Blue asterisks indicate significantly upregulated (fold change ≥ 1.5) genes (* for $FDR < 0.05$, ** for $FDR < 0.01$, *** for $FDR < 0.001$) as calculated from our differential expression testing results. (TNFα: tumor necrosis factor alpha, IFNγ: interferon gamma, IFNα: interferon alpha).
f. Heatmaps of CPZ demyelination (top) and remyelination (bottom) gene scores in mouse (upper panel) and human (lower panel) OL lineage cells. Each box is labeled with the total number of cells per condition, and conditions with fewer than 50 cells are shown in grey.

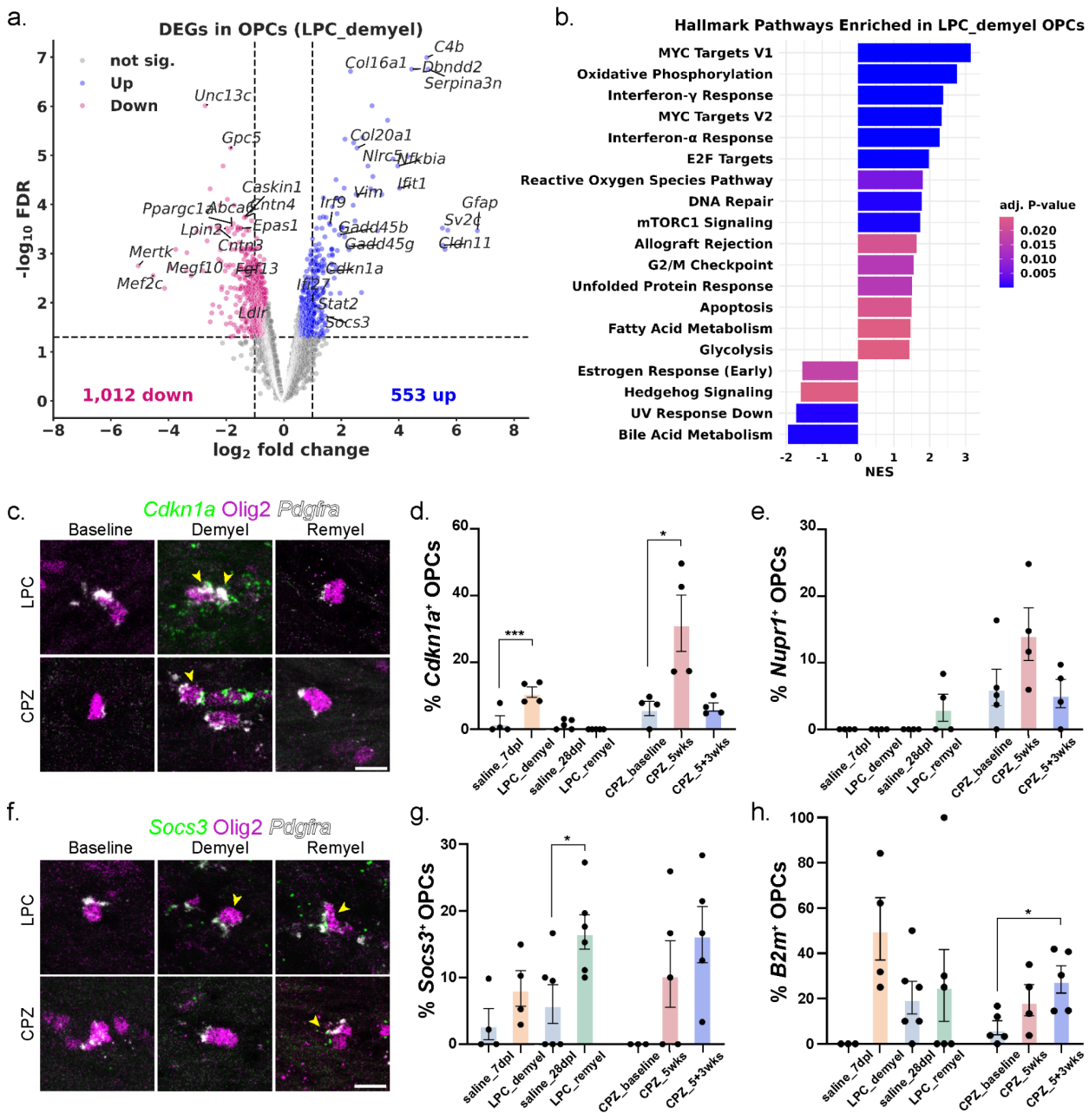
a.
DEGs in OPCs (LPC_demyel)
not sig.
Up
Down
1,012 down
553 up
-log10 FDR
log2 fold change
b.
Hallmark Pathways Enriched in LPC_demyel OPCs
MYC Targets V1
Oxidative Phosphorylation
Interferon-γ Response
MYC Targets V2
Interferon-α Response
E2F Targets
Reactive Oxygen Species Pathway
DNA Repair
mTORC1 Signaling
Allograft Rejection
G2/M Checkpoint
Unfolded Protein Response
Apoptosis
Fatty Acid Metabolism
Glycolysis
Estrogen Response (Early)
Hedgehog Signaling
UV Response Down
Bile Acid Metabolism
adj. P-value
NES
c.
Cdkn1a Olig2 Pdgfra
Baseline
Demyel
Remyel
LPC
CPZ
d.
% Cdkn1a+ OPCs
e.
% Nupr1+ OPCs
f.
Socs3 Olig2 Pdgfra
g.
% Socs3+ OPCs
h.
% B2m+ OPCs
saline_7dpl
LPC_demyel
saline_28dpl
LPC_remyel
CPZ_baseline
CPZ_5wks
CPZ_5+3wks

Supplementary Figure 9: Differential gene expression in OPCs from LPC and CPZ mouse models.

a. Volcano plot showing the statistical significance and logFC of all tested genes (each dot) for differential expression in OPCs following demyelination by LPC injection. Significantly upregulated genes are colored blue, and downregulated genes are colored magenta. Dashed horizontal and vertical lines indicate the significance thresholds for *padj* and logFC, respectively.
b. Bar chart showing the enrichment of Hallmark pathways from OPC gene expression at LPC demyelination. Color indicates the *padj*-value and bar length is the normalized enrichment score (NES).
c. Representative RNAscope images from the mouse corpus callosum showing *Cdkn1a* expression. Yellow arrows show *Cdkn1a*$^+$ OPCs. Timepoints for LPC are: baseline = saline-injected at 7 dpl, demyel = LPC injected at 7dpl, and remyel = LPC injected at 28 dpl; and for CPZ: baseline = normal diet, demyel = 5 weeks of CPZ chow, and remyel = 5 weeks CPZ chow and 3 weeks of recovery. (Scale bar = 10 μm).
d. Bar chart showing the percentage of *Cdkn1a*$^+$ OPCs across lesion conditions for n=4 (7 dpl, CPZ) and n=5 (28 dpl) animals. Bars represent group means, dots show individual animals, and error bars indicate SEM. Statistical significance was assessed by one-way ANOVA with Tukey's multiple comparisons test (***p = 0.0006, *p = 0.0154*).*
e. Bar chart showing the percentage of *Nupr1*$^+$ OPCs across lesion conditions for n=5 (CPZ_baseline) and n=4 (all other timepoints) animals. Bars represent group means, dots show individual animals, and error bars indicate SEM.
f. Representative RNAscope images from the mouse corpus callosum showing *Socs3* expression. Yellow arrows show *Socs3*$^+$ OPCs. Timepoints are the same as above. (Scale bar = 10 μm).
g. Bar chart showing the percentage of *Socs3*$^+$ OPCs across lesion conditions for n=4 (7 dpl), n=6 (28 dpl), n=3 (CPZ_baseline), n=5 (CPZ_5wks, CPZ_5+3wks) animals. Bars represent group means, dots show individual animals, and error bars indicate SEM. Statistical significance was assessed by one-way ANOVA with Tukey's multiple comparisons test (*p = 0.0347*).*
h. Bar chart showing the percentage of *B2m*$^+$ OPCs across lesion conditions for n=3 (saline at 7 dpl), n=4 (LPC at 7 dpl, CPZ_5wks), n=6 (28 dpl), n=3 (CPZ_baseline), n=5 (CPZ_baseline, CPZ_5+3wks). Bars represent group means, dots show individual animals, and error bars indicate SEM. Statistical significance was assessed by one-way ANOVA with Tukey's multiple comparisons test (*p = 0.0347*).*

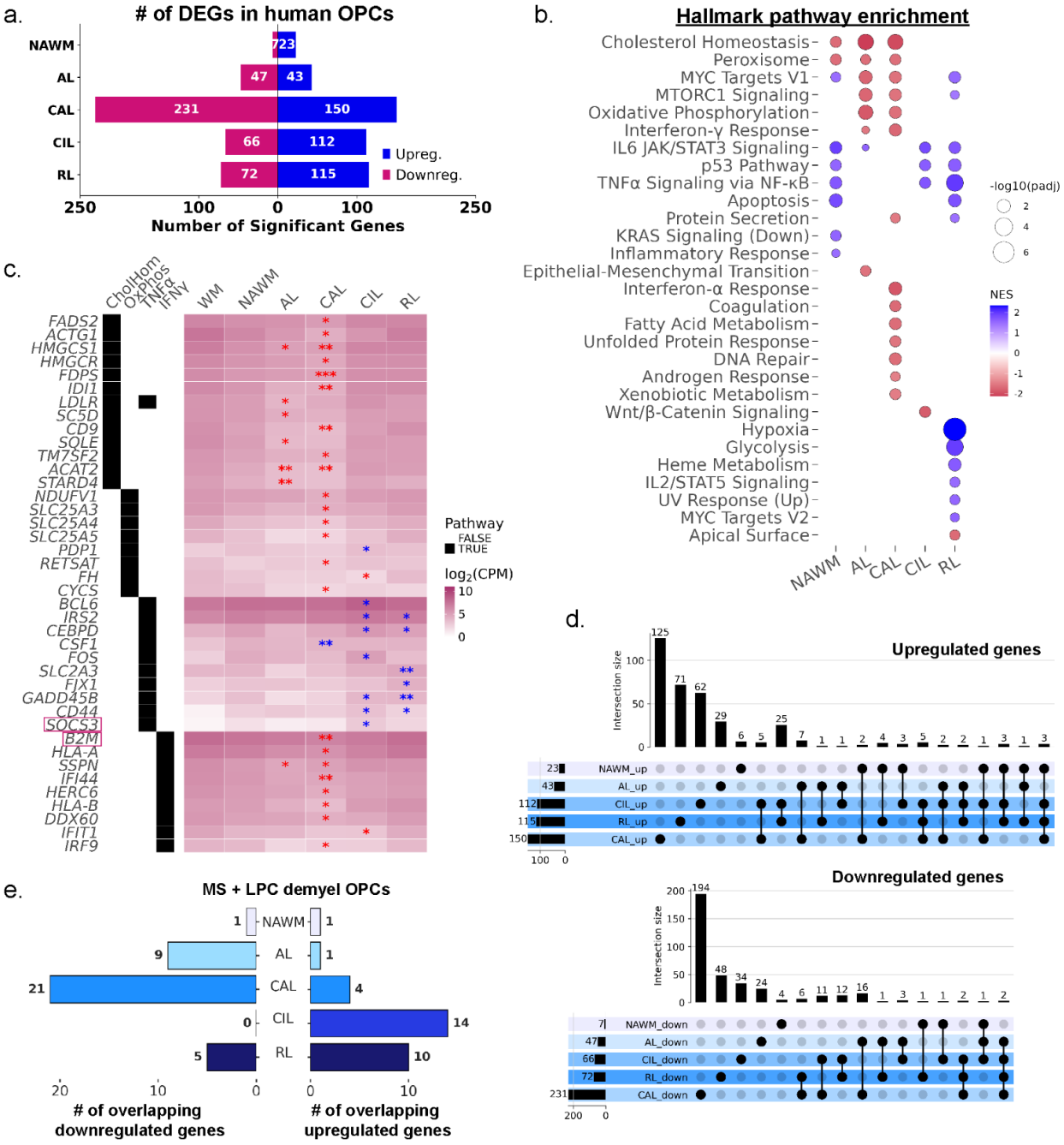

NAWM: *RAPGEF3*
AL: *LDLR, GPR158, SNCAIP, GPR155, CNTN4, VEGFA*
CAL: *HTRA1, OXR1, ACSL3 TMEM121, TMEM163, IDI1 PEX5L, EPN2, HMGCR, LRP1, TMEM241, PDGFRA, SCPEP1, MFSD8, NEU4, TMX4, LAPTM4B, ASAH1*
RL: *SHANK2, NKAIN3, MYT1L, XKR4*
AL/CAL: *HIP1R, INSIG1, MSMO1*
CAL/RL: *PEX5L*

NAWM: *SNRPN*
CAL: *CSF1, MRPS6, CLDN12, MOCS2*
CIL: *ADAMTS9, RNF220, BAIAP2, MAP1A, SNRPN, TUBB4A, GFAP, SOCS3*
RL: *TGFB2, LMNA, TP53, TNFRSF1A*
CIL/RL: *PROS1, GAP43, CEBPD, GADD45B*
AL/CIL/RL: *SNX10*

Supplementary Figure 10: OPC differential gene expression in humans and comparison between species.

a. Stacked bar chart showing the total number of upregulated (blue) and downregulated (magenta) DEGs across OPCs in each lesion type.
b. Dot plot showing the enrichment of Hallmark pathways per lesion type in OPCs. Dot color indicates normalized enrichment score (NES), and size reflects –log10(*padj*).
c. Heatmap showing the average $\log_2$-transformed CPM expression values of genes associated with the indicated pathways with significantly altered expression in at least one MS lesion condition in OPCs. Gene–pathway associations were assigned to pathways using the Hallmark sets and are shown in the left annotation panel, where black tiles indicate pathway membership. Genes are hierarchically ordered first by pathway inclusion and then by average expression across all conditions. Blue asterisks indicate significantly upregulated (fold change ≥ 1.5) genes and red asterisks indicate significantly downregulated (fold change ≤ –1.5) genes (* for *FDR* < 0.05, ** for *FDR* < 0.01, *** for *FDR* < 0.001) as calculated from our differential expression testing results. (CholHom: cholesterol homeostasis, OxPhos: oxidative phosphorylation, IFNγ: interferon gamma, TNFα: tumor necrosis factor alpha).
d. UpSet plots showing the unique (single points) and overlapping (connected points) DEGs in OPCs across lesion conditions that are upregulated (fold change ≥ 1.5, padj < 0.05, top) and downregulated (fold change ≤ –1.5, padj < 0.05, bottom).
e. Bar chart showing the overlap of upregulated (right) and downregulated (left) DEGs in OPCs between LPC at demyelination and the MS lesion types. Genes in boxes below the plots represent genes found in the unique overlap, or shared between mouse OPCs and multiple lesion types, as indicated.

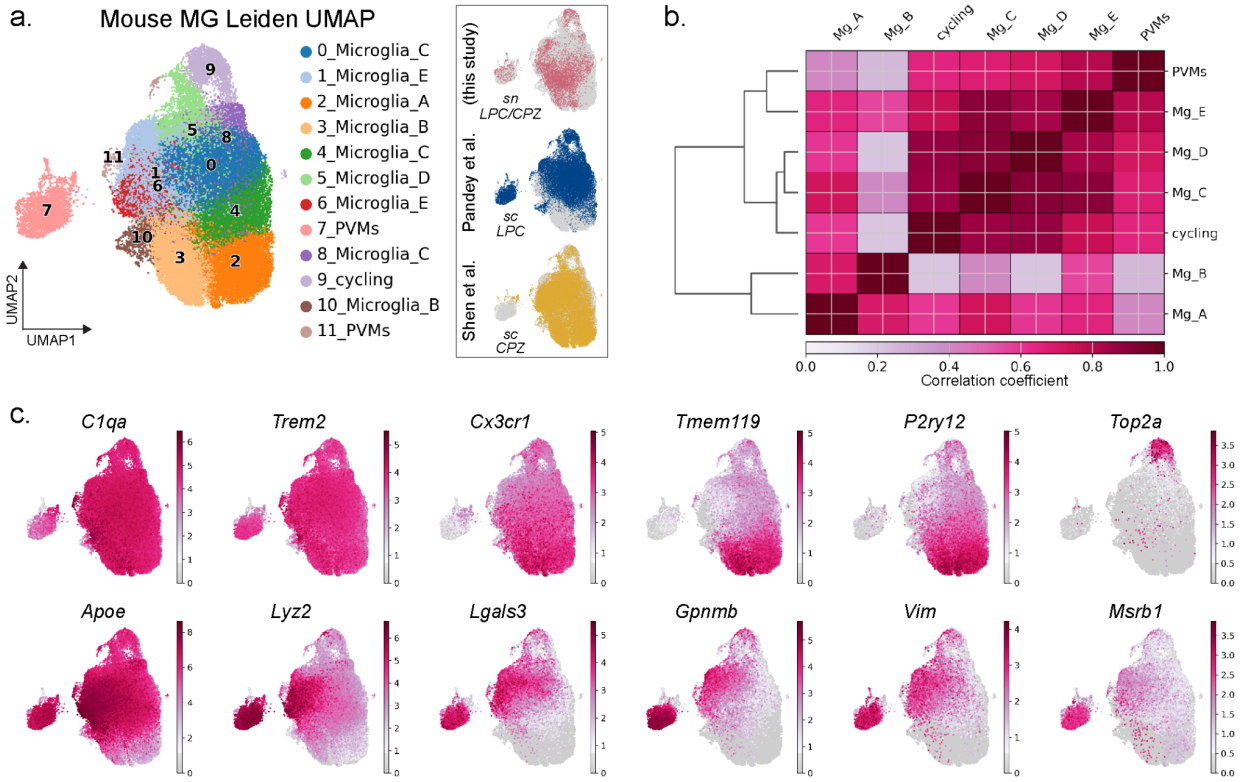
a.
Mouse MG Leiden UMAP
0_Microglia_C
1_Microglia_E
2_Microglia_A
3_Microglia_B
4_Microglia_C
5_Microglia_D
6_Microglia_E
7_PVMs
8_Microglia_C
9_cycling
10_Microglia_B
11_PVMs
UMAP1
UMAP2
(this study)
sn LPC/CPZ
Pandey et al.
sc LPC
Shen et al.
sc CPZ
b.
Mg_A
Mg_B
cycling
Mg_C
Mg_D
Mg_E
PVMs
Correlation coefficient
c.
C1qa
Trem2
Cx3cr1
Tmem119
P2ry12
Top2a
Apoe
Lyz2
Lgals3
Gpnmb
Vim
Msrb1

Supplementary Figure 11: Mouse microglia and PVM clustering and marker expression.

a. UMAP of the MG and PVM subset, with cell types labeled based on Leiden clustering. Inset UMAPs show samples separated and colored by dataset origin, labeled by the demyelination paradigm and sequencing type.
b. Correlation matrix and dendrogram showing the hierarchical clustering of the cell types.
c. UMAPs showing expression of the indicated marker genes, corresponding to the dot plot in Figure 5b.

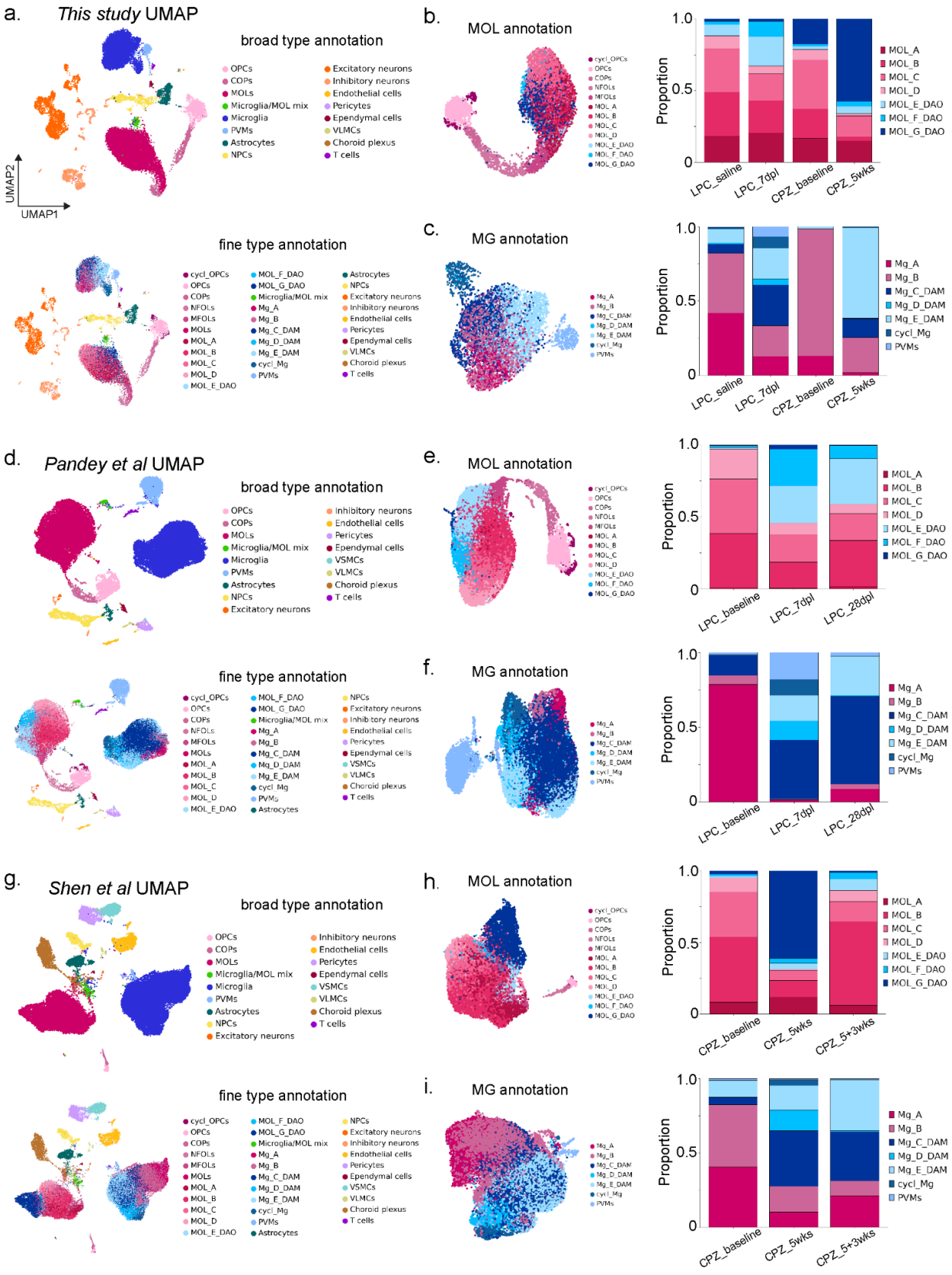
a.
This study UMAP
broad type annotation
OPCs
COPs
MOLs
Microglia/MOL mix
Microglia
PVMs
Astrocytes
NPCs
Excitatory neurons
Inhibitory neurons
Endothelial cells
Pericytes
Ependymal cells
VLMCs
Choroid plexus
T cells
UMAP2
UMAP1
fine type annotation
cycl_OPCs
OPCs
COPs
NFOLs
MFOLs
MOLs
MOL_A
MOL_B
MOL_C
MOL_D
MOL_E_DAO
MOL_F_DAO
MOL_G_DAO
Microglia/MOL mix
Mg_A
Mg_B
Mg_C_DAM
Mg_D_DAM
Mg_E_DAM
cycl_Mg
PVMs
Astrocytes
NPCs
Excitatory neurons
Inhibitory neurons
Endothelial cells
Pericytes
Ependymal cells
VLMCs
Choroid plexus
T cells
b.
MOL annotation
Proportion
1.0
0.5
0
LPC_saline
LPC_7dpl
CPZ_baseline
CPZ_5wks
c.
MG annotation
Mg_A
Mg_B
Mg_C_DAM
Mg_D_DAM
Mg_E_DAM
cycl_Mg
PVMs
d.
Pandey et al UMAP
e.
f.
LPC_baseline
LPC_28dpl
g.
Shen et al UMAP
CPZ_5+3wks
h.
i.

Supplementary Figure 12: QC of dataset integration and glial cell compositions.

a. Separate UMAP embedding of the single nucleus data generated in this study, colored by the broad cell types (top) and fine cell types (bottom), as shown in Figures 2 and 5.
b. Subset UMAP embedding of the OL lineage from the single nucleus data (left) and stacked bar chart showing the distribution of MOLs across conditions (right).
c. Subset UMAP embedding of the microglia and macrophage lineage cells from the single nucleus data (left) and stacked bar chart showing the distribution of these cell types across conditions (right).
d. Separate UMAP embedding of the single cell data generated in Pandey et al., colored as in (a).
e. Subset UMAP embedding (left) and stacked bar chart of cell types (right) of the OL lineage from Pandey et al as shown in (b).
f. Subset UMAP embedding (left) and stacked bar chart of cell types (right) of the microglia and macrophages from Pandey et al. as shown in (c).
g. Separate UMAP embedding of the single cell data generated in Shen et al., colored as in (a).
h. Subset UMAP embedding (left) and stacked bar chart of cell types (right) of the OL lineage from Shen et al. as shown in (b).
i. Subset UMAP (left) and stacked bar chart of cell types (right) of the microglia and macrophages from Shen et al. as shown in (c).

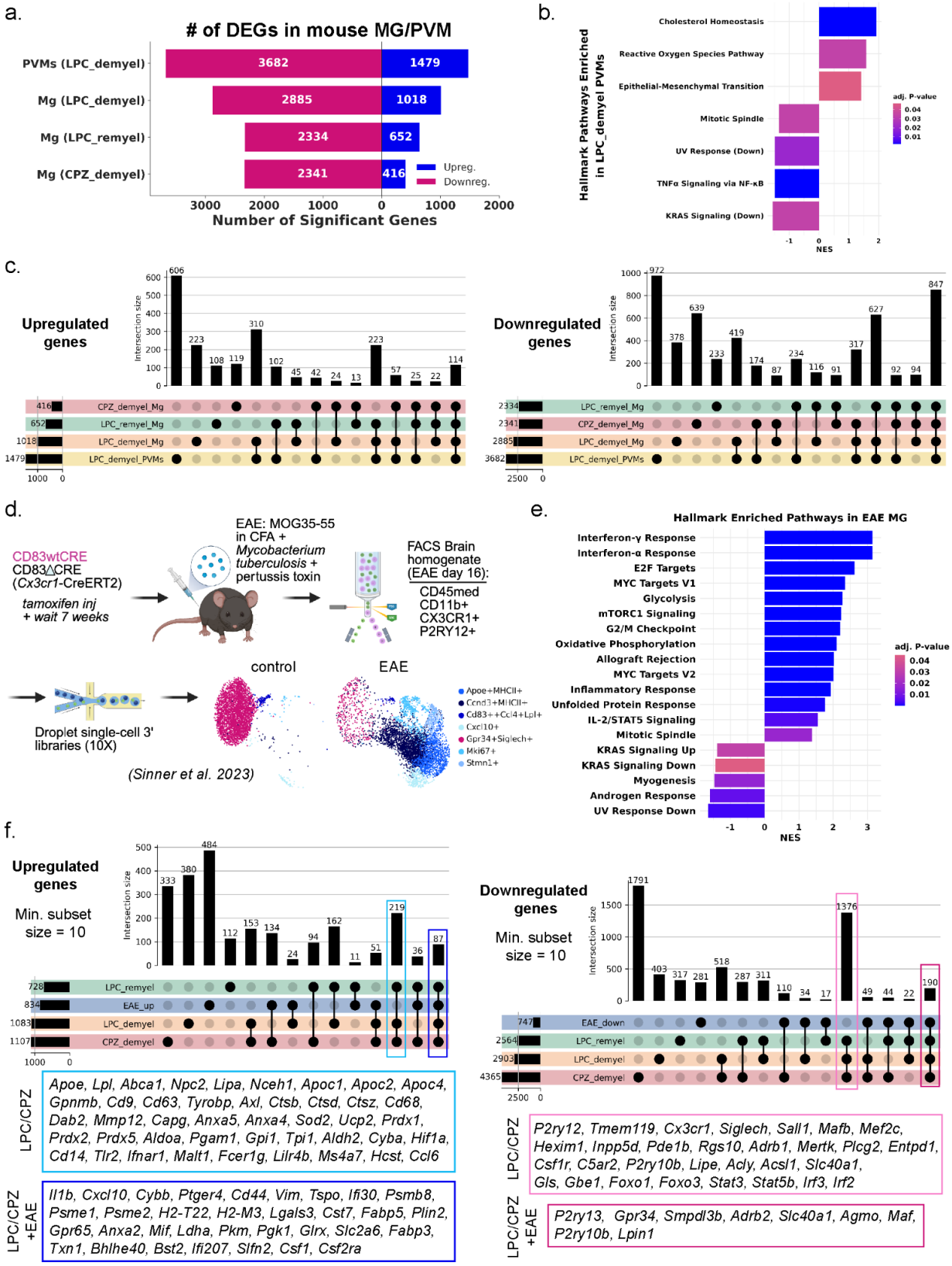
a.
# of DEGs in mouse MG/PVM
PVMs (LPC_demyel)
Mg (LPC_demyel)
Mg (LPC_remyel)
Mg (CPZ_demyel)
3682
1479
2885
1018
2334
652
2341
416
Upreg.
Downreg.
Number of Significant Genes
b.
Hallmark Pathways Enriched in LPC_demyel PVMs
Cholesterol Homeostasis
Reactive Oxygen Species Pathway
Epithelial-Mesenchymal Transition
Mitotic Spindle
UV Response (Down)
TNFα Signaling via NF-κB
KRAS Signaling (Down)
adj. P-value
NES
c.
Upregulated genes
Intersection size
CPZ_demyel_Mg
LPC_remyel_Mg
LPC_demyel_Mg
LPC_demyel_PVMs
Downregulated genes
LPC_remyel_Mg
CPZ_demyel_Mg
LPC_demyel_Mg
LPC_demyel_PVMs
d.
CD83wtCRE
CD83ΔCRE
(Cx3cr1-CreERT2)
tamoxifen inj
+ wait 7 weeks
EAE: MOG35-55
in CFA +
Mycobacterium
tuberculosis +
pertussis toxin
FACS Brain
homogenate
(EAE day 16):
CD45med
CD11b+
CX3CR1+
P2RY12+
Droplet single-cell 3'
libraries (10X)
control
EAE
Apoe+MHCII+
Ccnd3+MHCII−
Cd83+Ccl4+Lpl+
Cxcl10+
Gpr34+Siglech+
Mki67+
Stmn1+
(Sinner et al. 2023)
e.
Hallmark Enriched Pathways in EAE MG
Interferon-γ Response
Interferon-α Response
E2F Targets
MYC Targets V1
Glycolysis
mTORC1 Signaling
G2/M Checkpoint
Oxidative Phosphorylation
Allograft Rejection
MYC Targets V2
Inflammatory Response
Unfolded Protein Response
IL-2/STAT5 Signaling
Mitotic Spindle
KRAS Signaling Up
KRAS Signaling Down
Myogenesis
Androgen Response
UV Response Down
adj. P-value
NES
f.
Upregulated genes
Min. subset size = 10
Intersection size
LPC_remyel
EAE_up
LPC_demyel
CPZ_demyel
LPC/CPZ
Apoe, Lpl, Abca1, Npc2, Lipa, Nceh1, Apoc1, Apoc2, Apoc4, Gpnmb, Cd9, Cd63, Tyrobp, Axl, Ctsb, Ctsd, Ctsz, Cd68, Dab2, Mmp12, Capg, Anxa5, Anxa4, Sod2, Ucp2, Prdx1, Prdx2, Prdx5, Aldoa, Pgam1, Gpi1, Tpi1, Aldh2, Cyba, Hif1a, Cd14, Tlr2, Ifnar1, Malt1, Fcer1g, Lilr4b, Ms4a7, Hcst, Ccl6
LPC/CPZ +EAE
Il1b, Cxcl10, Cybb, Ptger4, Cd44, Vim, Tspo, Ifi30, Psmb8, Psme1, Psme2, H2-T22, H2-M3, Lgals3, Cst7, Fabp5, Plin2, Gpr65, Anxa2, Mif, Ldha, Pkm, Pgk1, Glrx, Slc2a6, Fabp3, Txn1, Bhlhe40, Bst2, Ifi207, Slfn2, Csf1, Csf2ra
Downregulated genes
Min. subset size = 10
EAE_down
LPC_remyel
LPC_demyel
CPZ_demyel
LPC/CPZ
P2ry12, Tmem119, Cx3cr1, Siglech, Sall1, Mafb, Mef2c, Hexim1, Inpp5d, Pde1b, Rgs10, Adrb1, Mertk, Plcg2, Entpd1, Csf1r, C5ar2, P2ry10b, Lipe, Acly, Acsl1, Slc40a1, Gls, Gbe1, Foxo1, Foxo3, Stat3, Stat5b, Irf3, Irf2
LPC/CPZ +EAE
P2ry13, Gpr34, Smpdl3b, Adrb2, Slc40a1, Agmo, Maf, P2ry10b, Lpin1

Supplementary Figure 13: Differential expression analysis of CPZ and LPC microglia and PVMs with comparison to EAE, revealing a conserved microglial program and broader transcriptional changes in toxin models.

a. Stacked bar chart showing the total number of upregulated (blue) and downregulated (magenta) DEGs in MG and PVMs compared to baseline per timepoint as indicated.
b. Bar chart showing the enrichment of Hallmark pathways from the gene expression changes in PVMs at LPC demyelination vs all microglia and PVM cells at LPC baseline. Color indicates the *padj*-value and bar length is the normalized enrichment score (NES).
c. UpSet plots showing the unique (single points) and overlapping (connected points) DEGs from PVM and microglia across lesion conditions that are upregulated (fold change ≥ 1.5, padj < 0.05, top) and downregulated (fold change ≤ –1.5, padj < 0.05, bottom).
d. Schematic of the EAE dataset used for microglia comparison. EAE was induced in transgenic adult mice, including negative controls (without knockdown) and microglia-specific CD83 knockdown animals. At 16 days post-induction, mice were sacrificed and total brain lysates were generated to isolate live cells. Microglia were FACS-sorted using the gene panel as listed, and subjected to scRNA-seq (10X genomics). UMAP of EAE-induced brain microglia colored by celltype, subset to negative controls (no gene knockdown) with and without EAE induction. (*Sinner et al. 2023)*. Created in Biorender. Aboelnour, E. (2026) https://BioRender.com/ik17ajo.
e. Bar chart showing the enrichment of Hallmark pathways in EAE-induced brain microglia. Color indicates the *padj*-value and bar length is the normalized enrichment score (NES). Full DEG outputs are supplied in the supplementary data.
f. UpSet plots showing the unique (single points) and overlapping (connected points) DEGs across microglia in the indicated EAE, LPC and CPZ conditions. Upregulated genes (fold change ≥ 1.5, padj < 0.05, top) are shown at left, and downregulated genes (fold change ≤ –1.5, padj < 0.05, bottom) at right. Representative genes for selected comparisons are highlighted in colored boxes below the corresponding plots.

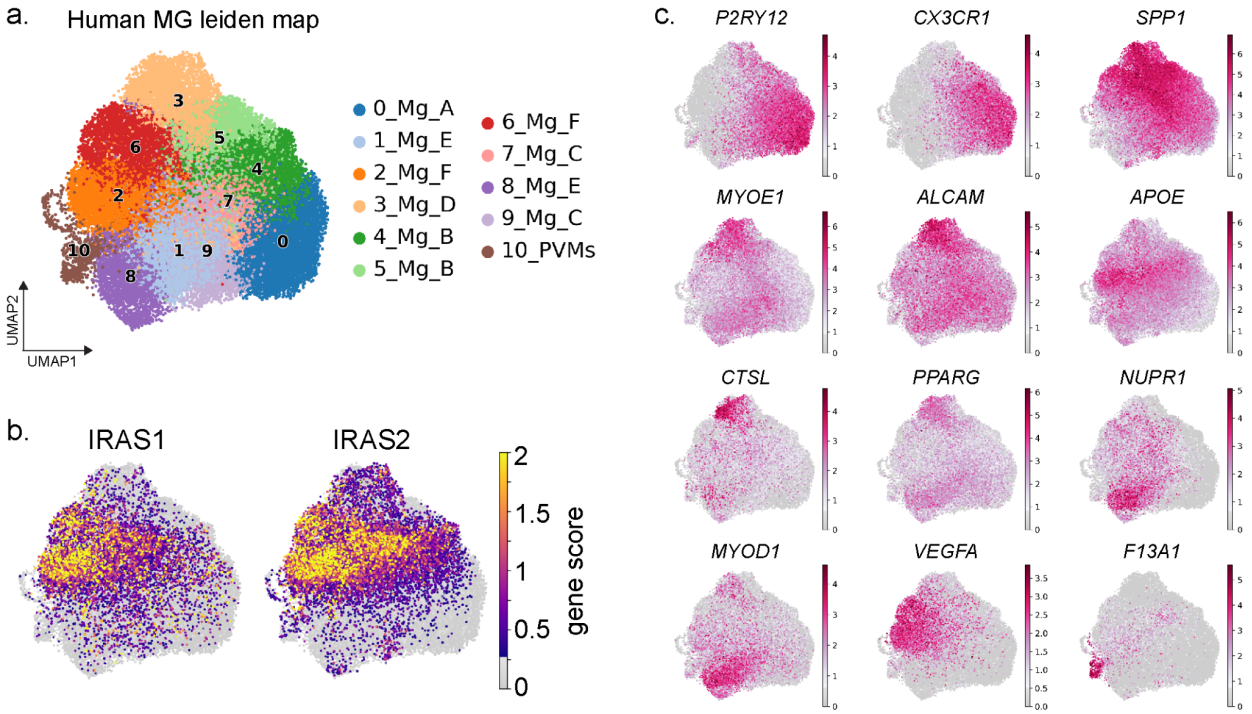
a.
Human MG leiden map
3
6
5
4
2
7
10
1
9
0
8
UMAP2
UMAP1
0_Mg_A
1_Mg_E
2_Mg_F
3_Mg_D
4_Mg_B
5_Mg_B
6_Mg_F
7_Mg_C
8_Mg_E
9_Mg_C
10_PVMs
b.
IRAS1
IRAS2
2
1.5
1
0.5
0
gene score
c.
P2RY12
CX3CR1
SPP1
MYOE1
ALCAM
APOE
CTSL
PPARG
NUPR1
MYOD1
VEGFA
F13A1

Supplementary Figure 14: Human microglia lineage clustering and marker expression.

a. UMAP of the human MG and PVM subset, with cell types labeled based on Leiden clustering.
b. UMAPs showing gene scores from Leng et al., based on inflammatory reactive astrocyte signatures: IRAS1 (enriched for MYC and mTORC signaling) and IRAS2 (enriched for IFN response genes).
c. UMAPs showing expression of the indicated marker genes, corresponding to the dot plot in Figure 6b.

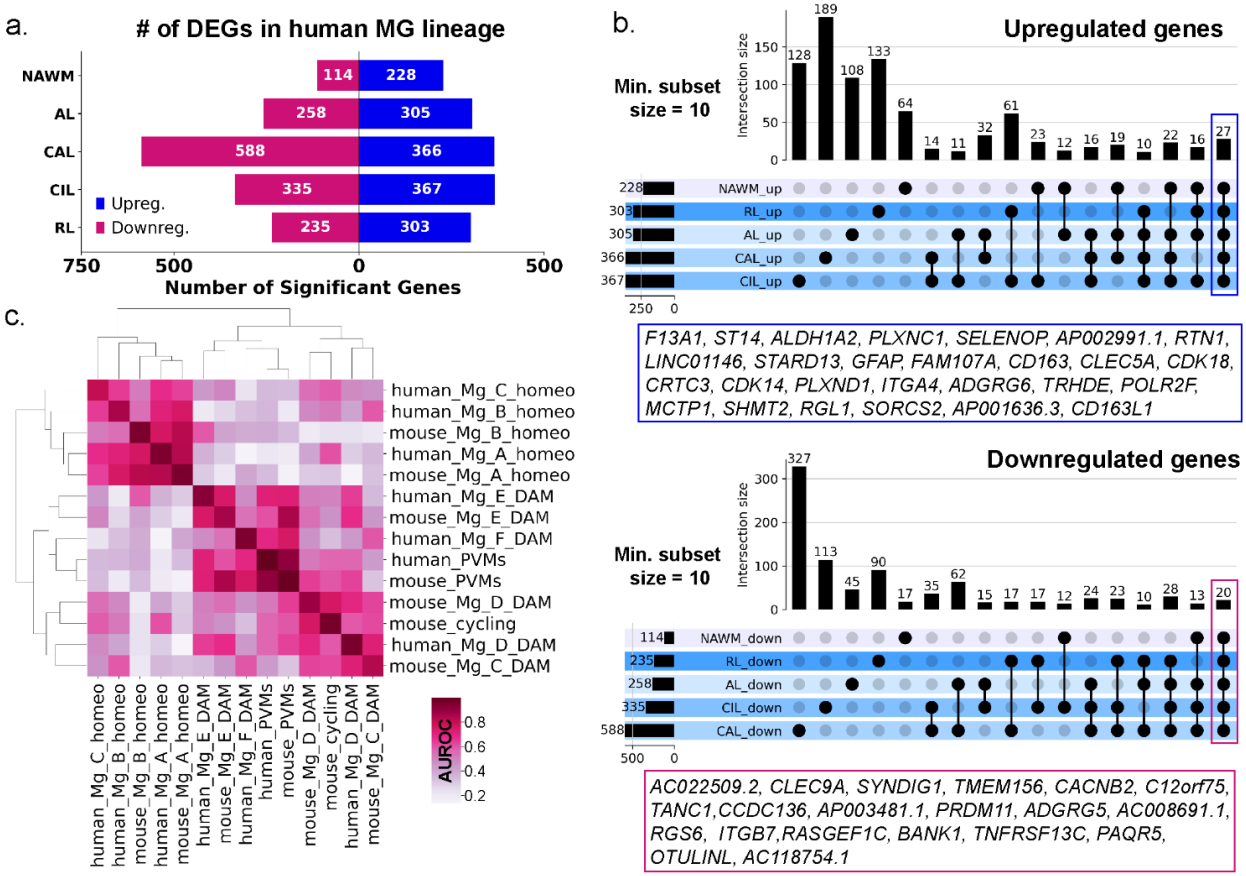
a.
# of DEGs in human MG lineage
NAWM
AL
CAL
CIL
RL
114
228
258
305
588
366
335
367
235
303
Upreg.
Downreg.
750
500
0
500
Number of Significant Genes
b.
Upregulated genes
Min. subset size = 10
Intersection size
128
189
108
133
64
14
11
32
61
23
12
16
19
10
22
16
27
NAWM_up
RL_up
AL_up
CAL_up
CIL_up
228
303
305
366
367
250
0
F13A1, ST14, ALDH1A2, PLXNC1, SELENOP, AP002991.1, RTN1, LINC01146, STARD13, GFAP, FAM107A, CD163, CLEC5A, CDK18, CRTC3, CDK14, PLXND1, ITGA4, ADGRG6, TRHDE, POLR2F, MCTP1, SHMT2, RGL1, SORCS2, AP001636.3, CD163L1
Downregulated genes
Min. subset size = 10
Intersection size
327
113
45
90
17
35
62
15
17
17
12
24
23
10
28
13
20
NAWM_down
RL_down
AL_down
CIL_down
CAL_down
114
235
258
335
588
500
0
AC022509.2, CLEC9A, SYNDIG1, TMEM156, CACNB2, C12orf75, TANC1,CCDC136, AP003481.1, PRDM11, ADGRG5, AC008691.1, RGS6, ITGB7,RASGEF1C, BANK1, TNFRSF13C, PAQR5, OTULINL, AC118754.1
c.
human_Mg_C_homeo
human_Mg_B_homeo
mouse_Mg_B_homeo
human_Mg_A_homeo
mouse_Mg_A_homeo
human_Mg_E_DAM
mouse_Mg_E_DAM
human_Mg_F_DAM
mouse_Mg_F_DAM
human_PVMs
mouse_PVMs
mouse_Mg_D_DAM
mouse_cycling
human_Mg_D_DAM
mouse_Mg_C_DAM
AUROC
0.8
0.6
0.4
0.2
d.
MS + LPC remyel
NAWM
AL
CAL
CIL
RL
14
32
52
39
112
26
47
42
45
32
40
20
0
0
20
40
# of overlapping downregulated genes
# of overlapping upregulated genes
P2RY12, CX3CR1, TMEM119, SALL1, MEF2C, EGR2, NLRP3, HAVCR2
APOE, LGALS3, GPNMB, LPL, FABP5, FYN, METRNL, TSPO, BCL3, SLAMF8
e.
Complement
Inflam
Hypoxia
Glycolysis
WM
NAWM
AL
CAL
CIL
RL
KYNU
PLA2G7
APOC1
ITA4H
FCER1G
PIM1
SERPING1
LGALS3
FYN
CR1
CLU
ABCA1
IL4R
NAMPT
IL15
SLC31A1
MXD1
SLC31A2
NOD2
AQP9
IL18R1
CCL20
IL10
IL1R1
GLRX
PAM
PLIN2
TGFBI
NFIL3
PGM1
VEGFA
FOSL2
RRAGD
NDRG1
SDC2
SDC3
PLAC8
B3GALT6
ISG20
ENO2
MERTK
PKM
PYGL
DSP
PKP2
STMN1
Pathway
FALSE
TRUE
log2(CPM)
15
10
5
0
f.
Hypoxia score
Inflamm score
LPC_baseline
LPC_demyel
LPC_remyel
CPZ_baseline
CPZ_demyel
Mg_A
Mg_B
Mg_C_DAM
Mg_D_DAM
Mg_E_DAM
PVMs
cycling
Gene set score
0.75
0.50
0.25
0.00
WM
NAWM
AL
CAL
CIL
RL
Mg_C
Mg_F_DAM

Supplementary Figure 15: Human microglia lineage DEG analysis.

a. Stacked bar chart showing the total number of upregulated and downregulated differentially expressed genes in MG per lesion condition compared to WM.
b. UpSet plots showing the unique (single points) and overlapping (connected points) DEGs in MG across lesion conditions that are upregulated (fold change ≥ 1.5, padj < 0.05, top) and downregulated (fold change ≤ –1.5, padj < 0.05, bottom). Overlap size was filtered to include only points with 10 or more shared genes.
c. Heatmap of AUROC scores between mouse and human MG lineage cells. Dendrograms were generated by hierarchical clustering of Euclidean distances using average linkage.
d. Bar chart showing the overlap of upregulated and downregulated DEGs shared between microglia at the LPC remyelination timepoint and the MS lesions. A subset of shared genes between LPC remyelination MG and at least one MS lesion type are shown beside the down and upregulated bars.
e. Heatmap showing expression of genes in the indicated pathways across lesion conditions. Heatmaps are colored by the average $\log_2$-transformed CPM expression values. Gene–pathway associations were assigned to pathways using the Hallmark sets and are shown in the left annotation panel, where black tiles indicate pathway membership. Genes are hierarchically ordered first by pathway inclusion and then by average expression across all conditions. Blue asterisks indicate significantly upregulated (fold change ≥ 1.5) genes (* for $FDR < 0.05$, ** for $FDR < 0.01$, *** for $FDR < 0.001$) as calculated from our differential expression testing results. (Inflam: Inflammatory Response).
f. Heatmaps of hypoxia (top) and inflammatory (bottom) gene scores in mouse (upper panel) and human (lower panel) MG and PVM cells. Each box is labeled with the total number of cells per condition, and conditions with fewer than 100 cells are shown in grey.